THE JOURNAL OF PHYSICAL CHEMISTRY B

ARTICLE

pubs.acs.org/JPCB

The Influence of the Stereochemistry of Alanine Residue on the Solid State Conformation and Crystal Packing of Opioid Peptides Containing D-Ala or L-Ala in Message Domain − XRD and NMR Study

Katarzyna Trzeciak-Karlikowska,[†] Anna Bujacz,[‡] Włodzimierz Ciesielski,[†] Grzegorz D. Bujacz,[‡] and Marek J. Potrzebowski*[,†]

[†]Centre of Molecular and Macromolecular Studies, Polish Academy of Sciences, Sienkiewicza 112, 90-363 Lodz, Poland

[‡]Institute of Technical Biochemistry, Technical University of Lodz, Stefanowskiego 4/10, 90-924 Lodz, Poland

ABSTRACT: In this work, an X-ray diffraction (XRD) and solid state NMR study of two tetrapeptides with different stereochemistry of alanine residue is presented using Tyr-(D-Ala)-Phe-Gly (**1**), an N-terminal sequence of opioid peptide dermorphin, and its biologically inactive analog Tyr-(L-Ala)-Phe-Gly (**2**). Single-crystal XRD proved that **1** crystallized under different conditions from exclusively one structure: a monoclinic crystal with $P2_1$ space group. In contrast, **2** very easily formed at least three crystallographic modifications, **2a** (monoclinic $P2_1$), **2b** (orthorhombic $P2_12_12$) and **2c** (tetragonal $P4_12_12$). Solid-state NMR spectroscopy was employed to investigate the structure and molecular dynamics of **1**, **2a**, and **2b**. By employing different NMR experiments (dipolar dephasing and PILGRIM) and an analysis of the ^{13}C principal elements of the chemical shift tensor (CST), it was proven that the main skeleton of tetrapeptides is rigid, whereas significant differences in the molecular motion of the aromatic residues were observed. Comparing current data with those of previous studies (*J. Phys. Chem. B* **2004**, *108*, 4535−4545 and *Cryst. Growth Des.* **2009**, *9*, 4050−4059), it can be assumed that an important preorganization mechanism anticipating the formation of peptide crystals containing D-Ala in sequence is the intramolecular CH−π interaction, which occurs for the amino acid with D stereochemistry. This effect may be responsible for the formation of only one crystallographic form of D-Ala peptides.

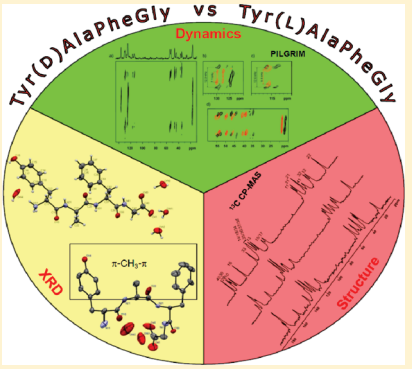

1. INTRODUCTION

In the 1970s, the first reports showing that peptides have biological properties and functions similar to those of opiates appeared.[1] The enkephalins (Tyr-Gly-Gly-Phe-Leu (Lenk) and Tyr-Gly-Gly-Phe-Met (Menk)), the first endogenous opioid peptide, were isolated and identified from a pig brain in 1975.[2] The discovery of opioid peptides have opened new perspectives in drug research. In particular, this class of compounds is promising for use as analgesics.[3]

In the early stage of biological studies, it was found that endogenous opioids are not very selective with respect to μ, δ, and κ receptors. Enkephalins are weak δ agonists, with selectivity ratios (δ/μ) slightly greater than unity. A much better selectivity was found for other opioid peptides from natural sources, deltorphin I (Tyr-D-Ala-Phe-Asp-Val-Val-Gly-NH_2), deltorphin II (Tyr-D-Ala-Phe-Glu-Val-Val-Gly-NH_2)[4,5] and dermorphin (Tyr-D-Ala-Phe-Gly-Tyr-Pro-Ser-NH_2),[6] which are found in the skin of South American frogs. They are very powerful δ- and μ-selective agonists, respectively. The presence of D-amino acid is crucial for biological activity. The synthetic analogues of given *supra* heptapeptides consisting of L-alanine are not analgesics.[7]

According to Schwyzer,[8] the OP sequences can be subdivided into two functional domain:, the recognition (or message) domain and the address domain. The message domain, common to most natural and synthetic opioid peptides, resides in the N-terminal part of the sequence and is necessary for recognition, whereas the address domain is responsible for selectivity and varies greatly among different opioids. In the cases of dermorphin and deltorphins, the message sequence consists of tyrosine, D-alanine, and phenylalanine, two adjacent aromatic residues separated by one amino acid with specific stereochemistry.

The crucial point in understanding the biological activity of opioid peptides is knowledge of the "bioactive shape" of the molecule and of the relative spatial positions of the functional groups.[9] The conformational analysis of opioid peptides is still important for receptor studies and drug design. To date, most conformational studies on dermorphin and deltorphins have used NMR spectroscopy.[10−14] It was indicated that the backbone conformation of the message sequence in solution is similar for both peptides, whereas a different orientation of the side chains is possible but not easily detected in the liquid phase.

The alternative approach in structural studies of flexible molecules is the analysis of solid-state structures. Although this

Received: June 14, 2011
Revised: July 4, 2011
Published: July 10, 2011

methodology has some limitations and may not reflect the conformational tendencies of isolated molecules because lattice forces are not negligible in many cases, low-energy conformations represent structures in the crystal lattice. In the case of opioid peptides containing D-amino acids, the question regarding the influence of the stereogenic center on bioactivity is still challenging.

In recent papers, the solid state structures and the influence of the alanine stereochemistry on crystal molecular packing and the internal dynamics of amino acids of the message sequence Tyr-Ala-Phe of dermorphin and deltorphins were reported using X-ray crystallography and NMR spectroscopy.[15,16] Continuing the structural study of opioid peptides, in this work, X-ray and NMR data are presented for tetra-peptides Tyr-Ala-Phe-Gly (N-terminal sequence of dermorphin) containing L-alanine and D-alanine in the sequence (Scheme 1). The NMR conformational study in a solution of tetrapeptides related to dermorphin has been reported elsewhere.[17]

2. EXPERIMENTAL SECTION

2.1. Synthesis of Tyr-D-Ala-Phe-Gly (1) and Tyr-L-Ala-Phe-Gly (2). The synthesis of Tyr-D-Ala-Phe-Gly (**1**) and Tyr-L-Ala-Phe-Gly (**2**) was carried out in solution according to a procedure[15,18] with the use of amino acids purchased from Sigma-Aldrich as starting materials.

2.2. X-ray Crystallography. Investigated compounds **1** and **2** were crystallized using the hanging drop technique by the vapor diffusion method. Peptide solutions at the concentration of 20 mg/mL were mixed with well solutions in a 3:1 ratio. The crystallization solution that grew **1** monoclinic crystals contained 3 M NaCl and 0.1 M Bis-Tris pH 5.5. The orthorhombic crystals **2b** were obtained in 3 M NaCl and 0.1 M Tris pH 8.5. The crystallization solution that grew **2c** tetragonal crystals contained 3 M NaCl and 0.1 M HEPES pH 7.5. The only exception referred the monoclinic form of **2** (labeled as **2a**) was crystallized in the batch method from a water−methanol mixture in a 2:1 ratio.

The monocrystals of all investigated forms were fished from the solution and, after removing crystallization buffers, mounted on the top of a small MicroMounts loop by using a thin layer of oil to force adhesion. The data of **1** were collected on the 14.2 beamline (BESSY, Berlin, Germany), using a MAR CCD 225-mm detector. The X-ray data of the monoclinic crystals of **2** were collected on the X13 beamline (EMBL-DESY Hamburg) using a MAR CCD 165 mm detector. The X-ray data of tetragonal and orthorhombic crystals of **2** were collected on a I911−2 beamline (MAX-Lab, Lund, Sweden) using a MAR CCD 165 mm detector. Due to the fixed wavelength and small detector diameter even at minimum crystal detector distance, the data resolution was only 0.95 A. The exposure time for a single frame corresponding to 1° of oscillation was 6, 10, 20, and 16 s for **1**, **2a**, **2b** and **2c**, respectively. The data were processed in HKL2000, with the exception of **2a**, where a change of orientation during data collection was observed and Agilent Technology software CrysAlisPro better handled this problem. Experimental details from data collection and refinement statistics are gathered in Table 1. All observed reflections with $I > 0\sigma(I)$ were used to solve the structure by direct methods and refined by full matrix least-squares using F's.[19,20] The structure of **1** was solved in monoclinic space group $P2_1$, and there were three forms of **2**: monoclinic $P2_1$, orthorhomic $P2_12_12$, and tetragonal $P4_12_12$ space groups.

Scheme 1. Structure of Model Compounds with Carbon Atoms Labeled

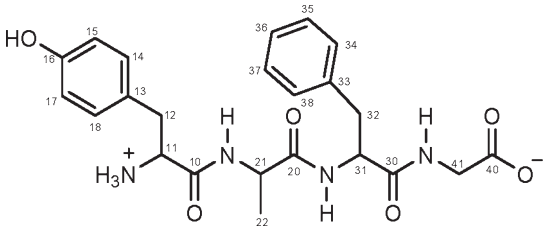

Hydrogen atoms connected to carbons were located geometrically and refined as a riding. H atoms connected to oxygen and nitrogen atoms were located on a difference Fourier map and were refined with restrained distances. The temperature factors for all hydrogen atoms were assigned to be 1.33 of the equivalent isotropic temperature factor of the parenting atom. Anisotropic thermal parameters were refined for all non-hydrogen atoms. In compound **1**, one of the two water molecules has two alternative positions. In compound **2a**, a single water molecule is present, but this molecule is disordered and modeled in three alternative positions. The structure **2b** has the highest water content with 5.5 molecules per one tetra peptide chain. The solvent area is very dynamic: only one water molecule in the special position is fully ordered, the next water molecule in the vicinity of the tyrosine hydroxyl group has two alternative positions, and the next four water molecules were modeled in three alternative positions in the equal occupancy in positions A, B, and C and complementary to one.

Usage of synchrotron radiation for structural analysis gave diffraction data for relatively small crystals and determined the crystal structure with better statistic parameters in comparison to data obtained on standard diffractometers. Crystal data were deposited in the Cambridge Crystallographic Data Centre under No.: 826341 (**1**), 826338 (**2a**), 826339 (**2b**), and 826340 (**2c**).

2.3. NMR Spectroscopy. The solid-state magic angle spinning (MAS) experiments were performed on a BRUKER Avance III 400 spectrometer at a frequency of 100.613 MHz for ^{13}C, equipped with an MAS probe head using 4 mm ZrO_2 rotors. A sample of glycine was used to set the Hartmann−Hahn condition, and glycine was used as a secondary chemical shift reference δ = 176.04 ppm from external trimethylsilane (TMS).[21] The conventional spectra were recorded with a proton 90° pulse length of 4 μs and a contact time of 2 ms. The repetition delay was 6 s, and the spectra width was 25 kHz. The free induction decays (FIDs) were accumulated with time domain size of 2 K data points. The RAMP shape pulse[22] was used during the cross-polarization and two-pulse phase modulation (TPPM) decoupling.[23] The spectral data were processed using the TopSpin program.[24]

For the Lee−Goldberg cross-polarization (LG-CP) period, the ^1H effective field strength was 50 kHz in all experiments, and the ^{13}C spin-lock field strengths were adjusted to the first-order sideband condition $\omega_{13C} = \omega_{1H\,eff} - \omega_r$. The spinning speed was 13 kHz and was regulated to ±3 Hz by a pneumatic control unit. Recycle delays varied from 1.5 to 4 s. The two-dimensional (2D) LG-CP experiments incremented the LG-CP contact time at a step of 16.28 μs.

At a spinning speed of 13 kHz, the dwell time for the evolution period was thus 19.23 μs. The maximum t_1 evolution time was typically about 1 ms. Only cosine-modulated data were collected.

Table 1. Crystal Data and Experimental Details of Tetrapeptides

	1	2a	2b	2c
Crystal Data				
molecular formula	$C_{23}H_{28}N_4O_6 \cdot 2H_2O$	$C_{23}H_{28}N_4O_6 \cdot H_2O$	$C_{23}H_{28}N_4O_6 \cdot 5.5H_2O$	$C_{23}H_{28}N_4O_6 \cdot 4H_2O$
formula weight	492.53	474.52	555.58	528.56
crystallographic system	monoclinic	monoclinic	orthorhombic	tetragonal
space group	$P2_1$	$P2_1$	$P2_12_12$	$P4_12_12$
a [Å]	4.905(1)	9.282(5)	9.484(2)	9.552(1)
b [Å]	13.469(3)	9.300(3)	31.624(6)	9.552(1)
c [Å]	19.124(4)	14.792(1)	10.464(2)	59.751(12)
β [°]	94.81(3)	103.75(1)	90.0	90.0
V [Å^3]	1259.0(4)	1240.2(1)	3138.4(1)	5451.7(16)
Z	2	2	4	8
D_c [g/cm^3]	1.299	1.271	1.176	1.288
μ [mm^{-1}]	0.140	0.124	0.245	0.262
Measurement Details				
X-ray source	BESSY BL_14.2 Berlin	DESY X-13 Hamburg	MAX_Lab I911−2 Lund	MAX_Lab I911−2 Lund
crystal dimensions [μm]	100 × 50 × 10	500 × 50 × 10	300 × 30 × 10	150 × 150 × 20
wavelength [Å]	0.82657	0.80150	1.0379	1.0379
maximum 2θ [°]	66.98	56.32	66.26	66.24
T_{meas}	100 K	100 K	100K	100 K
no. of images	360	360	160	180
$\delta\varphi$ [°]	1.0	1.0	1.0	1.0
resolution [Å]	40 - 0.75	20 - 0.85	30 - 0.95	30 - 0.95
data processing				
R_{merge} [%]	7.0 (20.4)	7.4 (38.7)	7.5 (11.9)	5.1 (7.7)
completeness [%]	99.5 (95.9)	98.8 (98.7)	90.9 (82.9)	99.6 (99.4)
no. of reflections	20976	14653	8837	20757
no. of unique reflections	3262	4189	2120	3402
redundancy	6.4 (4.2)	6.7 (6.6)	3.9 (3.0)	6.1 (4.8)
$I/\sigma\langle I\rangle$	27.24 (6.97)	8.40(1.97) [a]	27.93 (13.41)	39.14 (26.29)
Refinement Statistics				
No. of reflections: unique	3262	4189	2120	3351
with $I > 0\sigma(I)$	3253	4189	2113	3321
obs. with $I > 2\sigma(I)$	2927	3114	1991	3259
no. of parameters refined	320	332	435	367
largest diff. peak [eå$^{-3}$]	0.498	0.430	0.489	0.355
largest diff. hole [eå$^{-3}$]	−0.526	−0.283	−0.236	−0.377
shift/esd max	0.000	0.000	0.000	0.000
R_{obs}	0.0683	0.0885	0.0833	0.0541
wR_{obs}	0.1943	0.2490	0.2380	0.1354
S_{obs}	1.016	1.014	1.012	1.015
weighting coeff.[b] m	0.1273	0.1488	0.2500	0.1118
n	0.8861			1.8195
extinction coeff.[c] k	0.0542	0.0930		0.0388
$F(000)$	524	504	1188	2256

[a] $F/\sigma\langle F\rangle$ (data processed and the statistics produced by CrysAlisPro). [b] Weighting scheme $w = [\sigma^2(Fo^2) + (mP)^2 + nP]^{-1}$, where $P = (Fo^2 + 2Fc^2)/3$. [c] Extinction method SHELXL, extinction expression $Fc^* = kFc[1 + 0.001 \times Fc^2\lambda^3/\sin(2\theta)]^{-1/4}$.

Thus, a real Fourier transformation was performed on the t_1 data, yielding spectra with a symmetrized ω_1 dimension and showing the dipolar splittings. Because the t_1 time signal increases with increasing LG-CP contact time, the ω_1 dimension was processed using the baseline correction mode "qfil" in the TopSpin software, which subtracts a constant intensity from the time signals before Fourier transformation and yields spectra free of a dominant zero-frequency peak, giving the $^1H-^{13}C$ doublet.

A 5-π pulse 2D PASS scheme and a 2500 Hz sample spinning speed were used in the 2D experiments. The π-pulse length

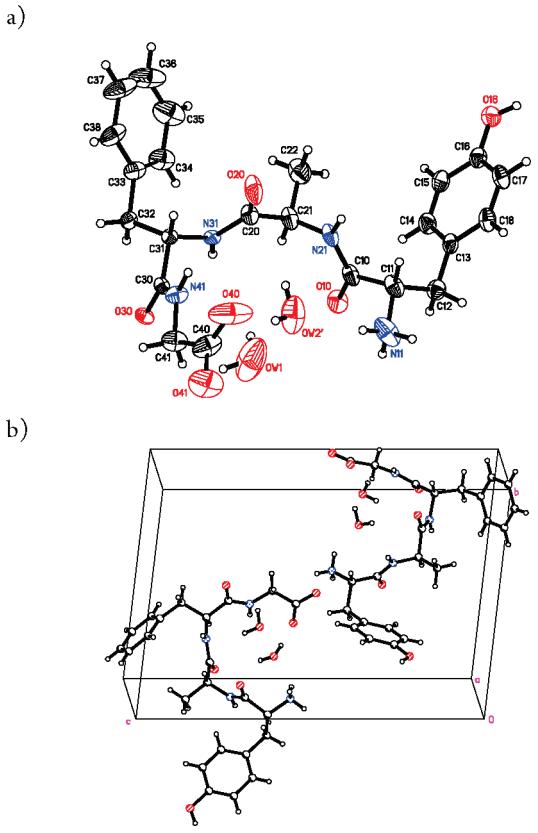

Figure 1. The crystal structure of Tyr-D-Ala-Phe-Gly (**1**): (a) ORTEP plot of one peptide molecule and two water molecules creating the independent unit (for disordered water, only the position with higher occupancy is shown); (b) the crystal packing of the unit cell.

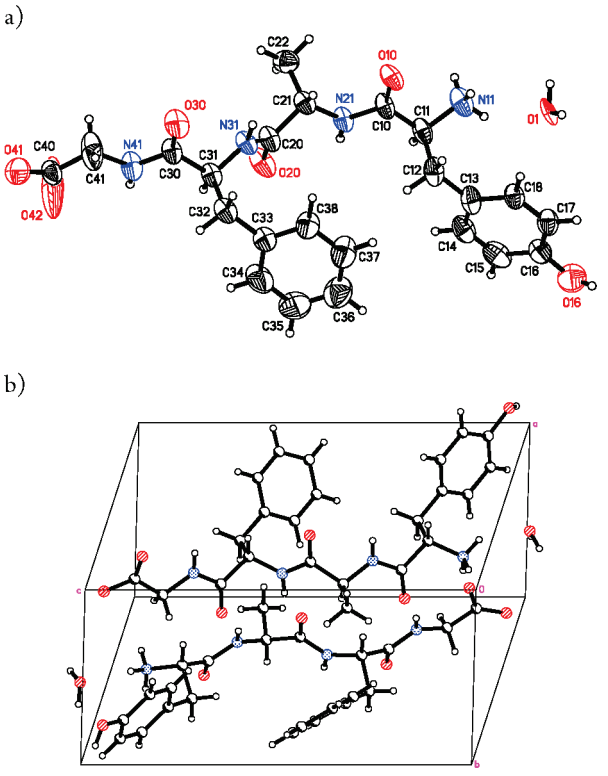

Figure 2. The crystal structure of Tyr-L-Ala-Phe-Gly (**2a**): (a) ORTEP plot of one peptide molecule and one disordered water molecule creating the independent unit (for disordered water, only the position with the highest occupancy is shown); (b) the crystal packing of the unit cell.

was 8 μs. Sixteen t_1 increments using the timings described by Levitt and co-workers were used in the 2D PASS experiments.[25] For each increment, 360 scans were accumulated. Because the pulse positions in the t_1 set go back to their original positions after a full cycle and the t_1-FID forms a full echo, the 16-point experimental t_1 data were replicated to 256 points. After the Fourier transformation in the direct dimension, the 2D spectrum was sheared so as to align all side bands with the center bands in the indirect dimension of the 2D spectrum. One-dimensional CSA spinning sideband patterns were obtained from t_1 slices taken at isotropic chemical shifts in the t_2 dimension of the 2D spectrum. The magnitudes of the principal elements of the CSA tensor were obtained from the best-fitting simulated spinning sideband pattern. Simulations of the spinning CSA side bands spectra were carried out on a PC using the TopSpin programs.

^{1}H 500 MHz Ultra Fast MAS NMR spectra recorded with the spinning rate 60 kHz were measured on a Bruker DRX spectrometer in 1.3 mm zirconium rotors with a $\pi/2$ pulse equal to 2.5 μs.

3. RESULTS AND DISCUSSION

3.1. X-ray Diffraction (XRD) Study of 1 and 2. *Sample* ***1*** *- Monoclinic form.* Sample **1** crystallizes in monoclinic space group $P2_1$. The asymmetric unit contains one tetra-peptide molecule and two molecules of water (Figure 1a). The packing of molecules in the unit cell is shown in Figure 1b. The peptide molecule has the "zwitter-ion" character, the N-terminal amino group is protonated, and the C-terminal carboxylic group is deprotonated. The overall shape of the main tetrapeptide chain is similar to the letter C. The N and C terminus groups interact with a disordered water molecule OW2. In both positions, it serves as a proton donor to the carboxyl group (2.30 Å and 2.36 Å, the distance between H2W and O40 in both positions, respectively) and as a proton acceptor to the amine group (1.76 Å and 2.09 Å, the distance between OW2 and H11A in both positions). The difference between them is the second hydrogen contact, where, for the first position, it occurs with the peptide oxygen group (2.94 Å distance between H1W′ and O20) and, in the second, with water OW1 (2.06 Å distance between H1W′′ and OW1). Two other hydrogen atoms of the ammonia moiety interact with the terminal carboxyl group of two symmetry related molecules and differ by an x translation. The H11B hydrogen atom interacts with both oxygen atoms O40 and O41 with distances 2.20 Å and 2.18 Å, respectively. The third hydrogen atom H11C interacts only with O41, creating a strong hydrogen bond of 1.90 Å. The second water molecule creates two hydrogen bonds: the first one between hydrogen H1W1 and oxygen O40 is equal to 1.93 Å, and the second between H2W1 and O20 is slightly weaker at 2.37 Å (both oxygens from the molecule related by translation along the x axis). The water molecules in the crystal create a water channel in the shape of a pipe running along the shortest b axis. The large part of that pipe is created by main chain peptide atoms and is closed by the edge of tyrosine side chains of symmetry related molecules.

Due to the D stereochemistry of the alanine residue, the hydrophobic side chains of tyrosine, phenylalanine, and alanine are located on the same side of the molecule. Together with the

dx.doi.org/10.1021/jp205570y |J. Phys. Chem. B 2011, 115, 9910–9919

symmetry related molecules, these residues create a hydrophobic interface, which is coplanar with the 110 plane of the crystal. The methyl group of alanine is located between four aromatic rings: two neighboring rings of tyrosine and phenylalanine from the same molecule and two phenylalanine rings from two symmetry related molecules. One of these rings is approximately perpendicular to the methyl group and able to create a CH$-\pi$ interaction with one of the methyl hydrogens with the distance from H22A to the center of the aromatic system equal to 3.79 Å. The hydrophilic interface created by the polar N and C terminus residues with the water molecules is located on a plane parallel to the hydrophobic one but translated by half of the **c** vector. The hydrogen of the tyrosine hydroxyl group creates a strong hydrogen bond with the carbonyl oxygen of the main chain of phenylalanine from the symmetry related molecule, with a length of 1.94 Å.

*Sample **2a** - Monoclinic Form.* The molecule of **2a** in monoclinic form has a β conformation. In this crystal form, the molecule creates an infinite β sheet in the 011 plane. The peptide chain is approximately parallel to the vector **c**, and the β sheet extends into the *b* cell edge. The β sheet is created by a network of hydrogen bonds: H11B···O42 1.76 Å, H41···O10 2.16 Å, H31···O20 2.00 Å, and O30···H21 2.15 Å. The first hydrogen bond is the strongest because it occurs between two charged terminal groups. The parallel β sheets create layers of molecules with a thin water interface between them. There is only one disordered water molecule per tetrapeptide (Figure 2a) molecule bridging the interactions between the terminal carboxyl and amino groups due to the two β sheet layers. Only one direct hydrogen bond between molecules from neighboring layers, namely H11C with O41 at a distance of 1.90 Å, is present. The packing of molecules in the unit cell is shown in Figure 2b.

In monoclinic form, the peptide molecules have angular orientation in respect to the layers, and the layer of solvent is located on the 110 plane. Two molecules of compound **2a** in the unit cell create a head-to-tail type of dimer. The disordered water molecule intermediates interactions between layers and creates direct hydrogen bonds with the C-terminal carboxyl group, the N-terminal amine group and the hydroxyl group of tyrosine. The methyl group of alanine is located in a cage formed by three phenylalanine and one tyrosine side chains. The last one is perpendicular to the methyl group and creates a weak CH-π interaction with the H22 distance to the center of the aromatic system equal to 2.89 Å.

*Sample **2b** - Orthorhombic Form.* The molecule of **2b** in orthorhombic form has a β conformation similar to molecules in monoclinic **2a.** In this crystal form, the molecule creates an infinite β sheet in the 110 plane. The peptide chain is approximately parallel to the vector **b**, and the β sheet extends into the *a* axis. The β sheet is created by an analogical network of hydrogen bonds as in the monoclinic form: H11C···O40 1.96 Å, H41···O10 2.23 Å, H31···O20 2.02 Å, O30···H21 2.05 Å. The crystal packing in the a cell direction is similar to the crystal packing in the **b** direction in the monoclinic form. The thickness of the solvent layer between layers of β sheets is much greater in the orthorhombic form than in monoclinic **2a**. The water "separator" allows the straight orientation of molecules in a layer. There is only one direct hydrogen bond between molecules in neighboring layers, namely H11B with O41 at a distance of 1.83 Å. There is also one ordered water molecule that interacts with the terminal carboxyl group located in a special position on the 2-fold axis. The distance H1A1···O41 is 1.91 Å. The rest of

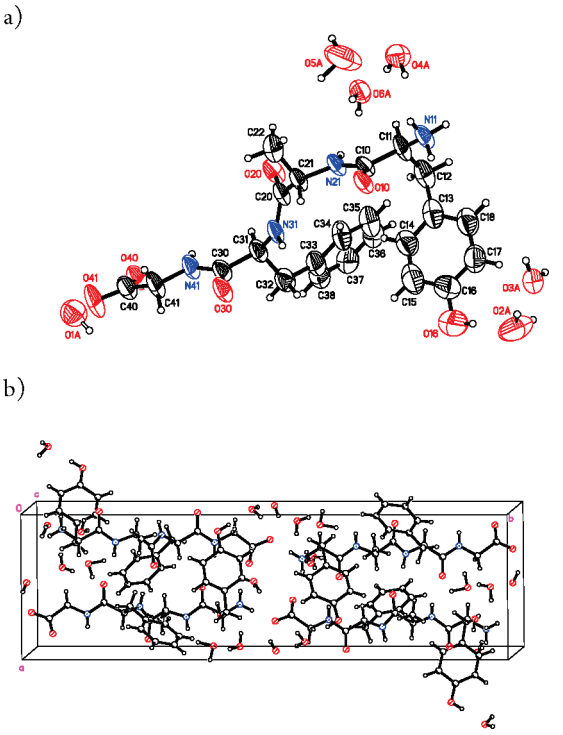

Figure 3. The crystal structure of Tyr-L-Ala-Phe-Gly (**2b**): (a) ORTEP plot of one peptide molecule and 5.5 water molecules creating the independent unit (for disordered water, only the position with the highest occupancy is shown); (b) the crystal packing of the unit cell.

the water molecules are disordered and create a water channel running along the *x* axis. The hydrophobic environment around the methyl side chain of alanine is also different. This group is located between two approximately perpendicular phenylalanine rings—the methylene group of the third phenylalanine and half of the tyrosine ring—all creating a hydrophobic hemisphere. One of the phenylalanine rings is approximately perpendicular to the C$\alpha-$Cβ bond and was able to create a CH$-\pi$ interaction with the H22B distance to the center of the aromatic system equal to 3.16 Å. It is interesting that the methyl group of alanine is exposed to the water channel from the other side of the hemisphere. Figure 3 shows the molecular structure (a) and the molecular packing (b) of sample Tyr-L-Ala-Phe-Gly (**2b**).

The difference between the monoclinic and the orthorhombic forms is due to the smaller number of water molecules between the layers of the tetrapeptide molecules. In the orthorhombic form, there are 5.5 water molecules in the asymmetric unit. In the monoclinic form, there is only one disordered water molecule.

*Sample **2c**- Tetragonal Form.* During the process of crystallization of **2** and the selection of material for X-ray measurements, new crystals labeled as **2c** were unexpectedly found, which can be produced only in a small amount during hanging drop crystallization. Due to the very small quantity of **2c** (not successfully produced on a larger scale), an NMR measurement could not be conducted.

The unit cell of the tetragonal form **2c** has a large *c* dimension, typical for protein crystals, and consists of eight molecules, with one monomer and four water molecules in the asymmetric unit. The independent peptide molecules exist in "zwitter-ionic" form with the positively charged terminals amine groups and deprotonated carboxylic groups. The main chain of the tetrapeptide

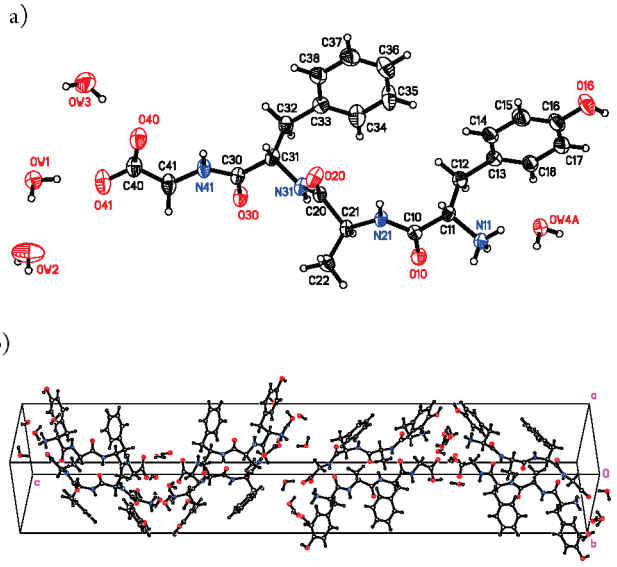

Figure 4. The crystal structure of Tyr-L-Ala-Phe-Gly (**2c**): (a) ORTEP plot of one peptide molecule and two four molecules creating an independent unit (for disordereed water, only the position with higher occupancy is shown); (b) the crystal packing of the unit cell.

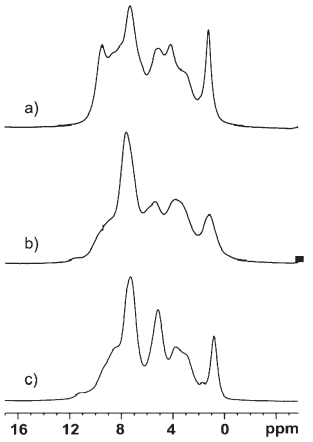

Figure 5. ^{1}H 500 MHz UF MAS NMR spectra of Tyr-Ala-Phe-Gly recorded at room temperature with a spinning rate of 60 kHz: (a) Tyr-D-Ala-Phe-Gly (**1**), (b) Tyr-L-Ala-Phe-Gly (**2a**), (c) Tyr-L-Ala-Phe-Gly (**2b**).

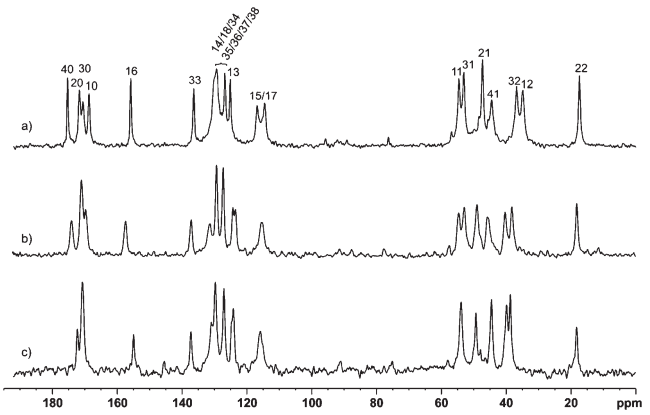

Figure 6. ^{13}C CP/MAS spectra of Tyr-Ala-Phe-Gly recorded at room temperature with a spinning rate of 8 kHz: a) Tyr-D-Ala-Phe-Gly (**1**), the assignment of ^{13}C resonances is shown, b) Tyr-L-Ala-Phe-Gly (**2a**) c) Tyr-L-Ala-Phe-Gly (**2b**).

has a natural typical β conformation. Symmetry related molecules create an infinite β sheet located in the plane *011*. The next layer of molecules is rotated by 90° and located in plane *101*. The β-sheet is created by hydrogen bonds: H11B···O40 1.90 Å, H41···O10 2.45 Å, H31···O20 2.04 Å, and O30···H21 2.2 Å. The first hydrogen bond is the strongest because it occurs between two charged terminal groups. Between the layers of molecules possessing β-sheet character, there is a layer of water molecules in plane *110* perpendicular to the *c* axis. Each water molecule in this layer has unique contacts. The oxygen of the OW1 is an acceptor for two protons from the tyrosine hydroxyl group and the ammonia group with distances of 1.77 Å and 1.95 Å, respectively. Both hydrogen atoms of this water molecule create hydrogen bonds with oxygen O41 from the terminal carboxyl group (1.83 Å) and oxygen OW2 of the next water molecule (1.95 Å). This water is also an acceptor tyrosine hydrogen proton H16···OW1 1.91 Å. The hydrogen atoms of OW2 create hydrogen bonds with the tyrosine main chain oxygen O10 (2.03 Å) and with the oxygen of the next water molecule OW3 (1.71 Å). The protons of the OW3 water interact with oxygen O40 of the terminal carboxyl group (1.98 Å) and the tyrosine hydroxyl oxygen O16 (2.01 Å). The last water molecule OW4 is disordered and, in both positions, serves as a donor of the ammonia proton H11A (1.90 Å and 1.99 Å). The hydrogen atoms of the water in first position interact with O41 and O16 with the distances 1.89 Å and 2.05 Å, respectively. The hydrogen atoms of the water in the second position interact with O41 and O41 (from the symmetry related molecules) with distances of 1.84 Å and 3.11 Å, respectively. The methyl group and two aromatic rings are located on the opposite side of the main chain and create hydrophobic contacts with phenyl rings from two neighboring phenylalanine residues in the β sheet. The hydrophobic environment is extended by the tyrosine and phenylalanine rings of the next molecule related by translation. Figure 4 shows the molecular structure (a) and the molecular packing (b) of **2c**. One of the phenylalanine rings is approximately perpendicular to the methyl group and creates a CH−π interaction with the distance from H22A to the center of the aromatic system equal to 2.86 Å.

The main difference between the **2a** and **2b** forms in comparison to the tetragonal **2c** is that, in the first two peptides, all β sheets have the same direction but, in the tetragonal form, every second layer is rotated by 90°. Due to the extended β-conformation in all crystal forms of **2**, the main chain torsion angles have very similar values. The side chain conformations are different in all crystal forms. The main difference is the χ1 torsion angle of the tyrosine molecule, which is 67.36° in the orthorhombic form and −75.53° and −61.23° in the tetragonal and the monoclinic crystal forms, respectively. The phenylalanine side chain has a very similar χ1 torsion angle but differs in χ2 in various crystal forms.

3.2. ^{1}H Ultra Fast MAS and ^{13}C CP/MAS NMR Study of 1 and 2a, 2b. ^{1}H solid state (SS) NMR spectra for **1** and **2** recorded under MAS with a 60-kHz spinning rate are displayed in Figure 5. ^{1}H SS NMR spectroscopy is very challenging because of extremely strong homonuclear dipolar coupling, which, in many cases, exceeds the range of the chemical shifts for protons.[26] The broadening of the proton lines is not removed by slow MAS. Therefore, the spectra recorded under slow conditions are

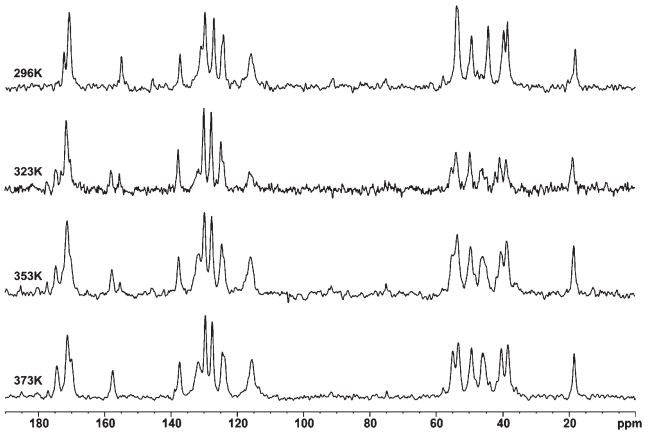

Figure 7. VT (296−373K) ^{13}C CP/MAS NMR spectra of Tyr-L-Ala-Phe-Gly (**2b**).

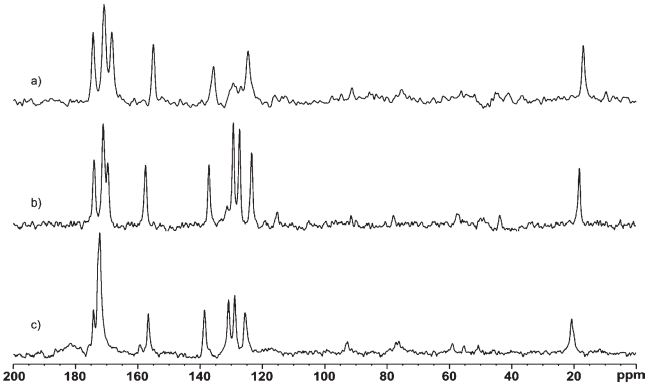

Figure 8. DD spectra of Tyr-Ala-Phe-Gly recorded with a dipolar delay equal to 50 μs: (a) Tyr-D-Ala-Phe-Gly (**1**), (b) Tyr-L-Ala-Phe-Gly (**2a**), (c) Tyr-L-Ala-Phe-Gly (**2b**).

difficult to analyze and usually do not contain subtle structural information. The "ultrafast" (UF) regime of more than 60 kHz is obtained using commercially available 1.3-mm rotors. This frequency exceeds the strength of the homonuclear proton dipolar coupling and is therefore expected to enter a new regime for spin dynamics.

From analysis of the spectra (Figure 5), the distinction between crystals of **1**, **2a**, and **2b** is apparent. For sample **1**, the resonance lines are relatively sharp and resolved. The resolution for samples **2** (Figure 5b,c) in the aliphatic region is slightly worse because signals in the aromatic region are averaged. The most striking difference between **2a** and **2b** is the strong signal at δ = 5.0 ppm (Figure 5a) representing the water molecule in the crystal lattice of **2b**. It is interesting to note that, during storing of sample **2b** at ambient temperature, the water signal gradually became smaller, and, after a few weeks, the spectrum of **2b** was very similar to that of **2a**. This problem will be further discussed below.

Figure 6 displays the ^{13}C CP/MAS NMR spectra of **1** and **2a, 2b** recorded at room temperature with a spinning rate of 8 kHz. ^{13}C resonances for sample **1** (Figure 6a) are sharp and well resolved. The ^{13}C CP/MAS spectra for tetrapeptides **2**, in particular in the carbonyl/carboxyl region, are not as high a quality as for **1**. The signals are overlapped and broadened. The

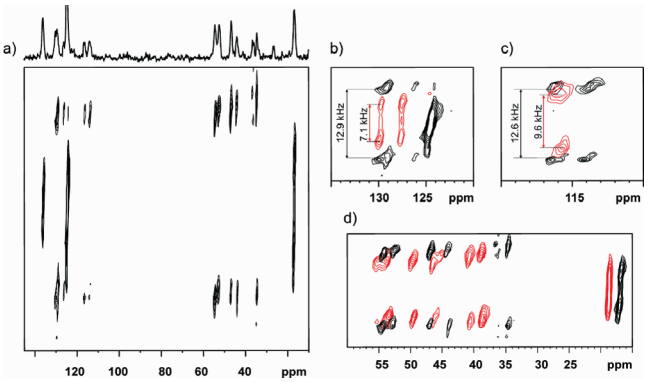

Figure 9. 2D PILGRIM spectrum of Tyr-Ala-Phe-Gly: (a) Tyr-D-Ala-Phe-Gly (**1**); (b) comparison of aromatic region for phenylalanine resonance of **1** (black) and **2b** (red); (c) comparison of aromatic region for tyrosine resonances of **1** (black) and **2b** (red), (d) comparison of aliphatic region of **1** (black) and **2b** (red).

resonances representing the C15/C17 tyrosine both for **2a** and **2b** are averaged. The distinction of chemical shifts for aliphatic signals is seen.

As shown *supra*, the **2b** crystals are unstable and, due to the release of water, undergo slow rearrangement at room temperature. This process can be confirmed employing ^{13}C CP/MAS measurements at variable temperatures (VT). Figure 7 shows ^{13}C (VT) CP/MAS spectra of **2b** measured in the temperature range from 296 to 373 K. The thermal transition of **2b** is apparent and consistent with ^{1}H UF MAS data. The region of 150−160 ppm (C16 carbons) is diagnostic and can be used to follow the progress of the transition. This process is nonreversible. With the removal of water from the hydrophobic channel, the ^{13}C spectrum of **2b** is similar to that of **2a**.

3.3. Solid-State NMR Study of Molecular Dynamics for 1 and 2. It is well-known that polymorphs of opioid peptides can differ in flexibility and represent different modes of molecular dynamics.[27] The methodology used for the analysis of the motional regime and geometry of molecular motion of peptides and proteins was exhaustively discussed by Krushelnitsky and Reichert.[28]

In the current project, as a preliminary test for the study of internal molecular motion for **1** and **2**, a dipolar dephasing (DD) pulse sequence was used.[29−31] This method is often used as a spectral editing technique. In the simplest approach after CP, the ^{1}H decoupler is turned off for approximately 50 μs, which is sufficient time for ^{13}C−^{1}H dipolar coupling to dephase the transverse magnetization of any ^{13}C isotope with a directly bonded ^{1}H isotope, as long as the dipolar coupling is not motionally averaged. In the case of sample **1** (Figure 8a), the lines for rigid CH and CH_2 are effectively suppressed while quaternary signals are observed. The methyl group is under a fast exchange regime, and its signal is only attenuated.

Figure 8b shows the spectrum for sample **2a**, which was recorded under exactly the same conditions as Figure 8a. For a dipolar delay equal to 50 μs, aromatic signals of phenylalanine are not suppressed. According to a statement given *supra*, it can be assumed that the phenyl ring is under a fast exchange regime. A similar conclusion is valid for sample **2b** (Figure 8c). Thus, the tetrapeptides **1** and **2** differ not only in molecular packing but also in molecular dynamics.

Further results regarding the distinct dynamics of the systems were obtained by employing dipolar recoupling experiments,

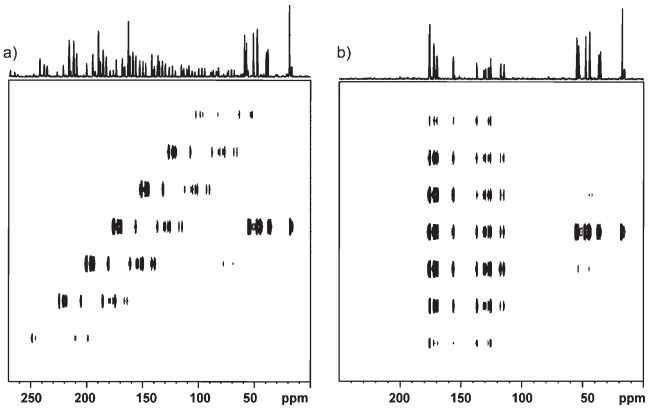

Figure 10. 2D PASS spectra for **1**: (a) recorded with a spinning rate of 2.5 kHz and (b) after data shearing.

which are well suited for measuring motional averaging at multiple sites simultaneously in biomolecules.[32−34] In 2D experiments, separated local field sequences can reintroduce dipolar anisotropic interactions and correlate them to isotropic chemical shifts.[35] The LG-CP[36,37] and polarization inversion spin exchange at the magic angle (PISEMA)[38] pulse sequences were recently used to correlate the motionally average anisotropic dipolar interactions with high-resolution chemical shift dimensions during MAS in a 2D approach.

In this work, for analysis of the effect of molecular motion on the line shape of the dipolar spectra, sensitivity-enhanced LG-CP measurements were conducted, employing the PILGRIM pulse sequence (*p*hase-*i*nverted *LG r*ecoupl*i*ng under *M*AS).[39] Compared to standard LG-CP, the theoretical sensitivity enhancement factor for PILGRIM is equal (2) (in practice, less). The applicability of the PILGRIM approach for the study of molecular dynamics of polymorphs of phenylalanine with static and flexible phenyl rings was discussed in the cited work.

As revealed elsewhere,[38,40] fast molecular motion can reduce the principal component of the dipolar tensor by factor (S), which is called the order parameter. For powder patterns, S is in range from 0.5 to 1. The latter value represents a rigid system. The order parameters related to dynamic models, including diffusion in a cone and the three-site hop for aliphatic groups and two-site jumping or diffusion in a flattened cone typical for dynamics of phenyl rings, have been reported. For a $^{13}C-^{1}H$ r_{ij} distance equal to 1.09 Å, δ, the dipolar coupling constant for the rigid limit, is 22.7 kHz, according to the following equation:

$$\delta = -\frac{\mu_0 \hbar^2}{4\pi} \frac{\gamma_i \gamma_j}{r_{ij}^3}$$

For the LG-CP experiment, the line shapes resemble a Pake pattern without the outer two "shoulders" and with splitting between singularities equal to a factor of 0.58 ($\cos \Theta_m$). For static phenyl rings, the splitting is 13.2 kHz. The molecular motion averages the dipolar coupling δ and changes the line shape.

Figure 9a shows the 2D PILGRIM spectrum for sample **1** recorded with a spinning rate of 13 kHz at ambient temperature. Under similar conditions were recorded spectra for **2a** and **2b**. Comparative analysis of overlapped spectra in the aromatic region for **1** and **2b** (Figure 9b) shows that phenyl rings for both samples are under dramatically different motional regimes.

Table 2. ^{13}C δ_{ii} Parameters Obtained from the 2D PASS Experiment, Fitted Using the TopSpin and WINMAS Programs[a]

carbon no.	δ_{iso} [ppm]	δ_{11} [ppm]	δ_{22} [ppm]	δ_{33} [ppm]	Ω [ppm]	κ [ppm]
Tyr-D-Ala-Phe-Gly (**1**)						
15/17	116	195 ± 4	132 ± 3	25 ± 2	170	0.28
35/37	127	221 ± 3	142 ± 2	20 ± 1	201	0.22
Tyr-Ala-Phe-Gly (**2a**)						
15/17	117	183 ± 7	131 ± 5	37 ± 2	146	0.29
35/37	130	203 ± 6	159 ± 5	29 ± 1	174	0.49
Tyr-Ala-Phe-Gly (**2b**)						
15/17	117	172 ± 5	149 ± 5	27 ± 1	145	0.66
35/37	130	204 ± 6	144 ± 4	51 ± 3	153	0.27

[a] The ^{13}C δ_{ii} parameters are defined as follows: $\delta_{11} \geq \delta_{22} \geq \delta_{33}$. The estimated error in δ_{iso} is ca 0.2 ppm; $\delta_{iso} = (\delta_{11} + \delta_{22} + \delta_{33})/3$, span is expressed as $\Omega = \delta_{11} - \delta_{33}$, and skew is expressed as $\kappa = 3(\delta_{22} - \delta_{iso})/\Omega$.

For **1**, the splitting is equal to 12.9 kHz, whereas, for **2b**, it is only 7.1 kHz. The order parameter S for phenyl ring of **2b** is equal to 0.54, and it is 0.98 for **1**. The splitting for aromatic resonances of tyrosine for **1** and **2b** are slightly different (Figure 9c): 12.6 kHz and 9.6 kHz, respectively. The appropriate S parameters are found to be 0.95 and 0.73. The analysis of the cross-peaks for aliphatic resonances shown in Figure 9d revealed that the main skeleton of the tetrapeptide is rather rigid with splitting values equal to 12.5 kHz. On the other hand, the methyl groups for both samples are under the fast molecular motion regime although slightly different.

3.4. ^{13}C 2D PASS Analysis of the CST Parameters for 1 and 2. Solid state NMR is a technique that provides detailed information not only about the structure but also about time scale of the dynamics processes and their geometry.[41] The most common approach for the study of the geometry of molecular motion is the line shape analysis of ^{2}H NMR static spectra.[42] Unfortunately, for such experiments, selectively labeled models are desired. Another complementary source of information is the analysis of the static line shape of ^{13}C nuclei. However, as in the previous case, this technique at natural abundance of ^{13}C nucleus provides unambiguous data for relatively simple systems. For the more complex compounds under investigation, for assigning of values of the principal elements ^{13}C δ_{ii} (ii = 11, 22, 33) of the chemical shift tensor (CST), which define the line shape, 2D NMR techniques can be employed. For rotating solids, ^{13}C δ_{ii} parameters can be obtained from the analysis of spinning sideband intensities. There are several approaches that allow the separation of the isotropic and anisotropic parts of the spectra with heavy overlapped systems.[43] In this work, the 2D PASS sequence was used for analysis of the ^{13}C spectra.[25] This technique offers good sensitivity compared to other methods and does not require hardware modifications or a special probehead.[44]

Figure 10a displays the 2D PASS spectrum for **1** recorded at a 2.5 kHz spinning rate. A similar procedure was employed to study of **2a** and **2b**. In general, the carbonyl groups and aromatic atoms are characterized by large CSA, and the spectra present a complex pattern under slow sample spinning. Using proper data shearing (Figure 10b), it is possible to separate the spinning sidebands for each carbon and to use a calculation procedure to

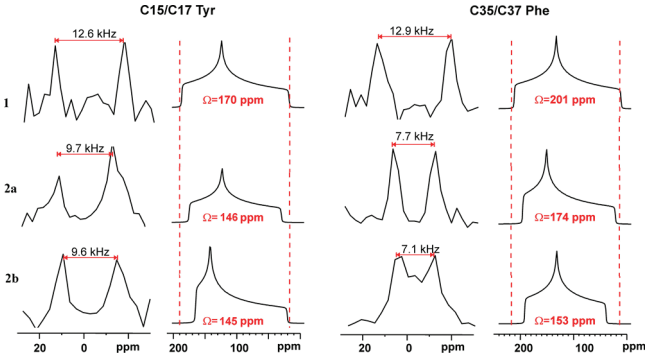

Figure 11. Comparison of the line-shapes for samples **1** (upper row), **2a** (middle row), and **2b** (bottom row). First and third columns show F1 projections taken from PILGRIM correlation (Figure 10) for tyrosine (C15/C17) and phenylalanine (C35/C37) carbons. Second and fourth columns present the calculated static ^{13}C line shape employing ^{13}C δ_{ii} values collected in Table 2.

establish the ^{13}C δ_{ii} parameters. It is clear that the F2 projection corresponds to the TOSS[45] spectrum, whereas F1 represents CSA. In this work, the focus was on only the aromatic signals of C35/C37 phenylalanine and C15/C17 resonances of tyrosine, which can be unambiguously assigned. For fitting of the spinning sideband pattern of F1 spectra, a procedure reported in previous papers was employed.[16] The values of selected ^{13}C δ_{ii} parameters for **1** and **2** are collected in Table 2.

In this part of the project, data obtained from $^{1}H-^{13}C$ recoupling experiments versus the line shape of the appropriate ^{13}C spectra were correlated. Figure 11 (first and third columns) shows F1 projections taken from the PILGRIM correlation (Figure 10) for tyrosine (C15/C17) and phenylalanine (C35/C37) carbons of samples **1**, **2a**, and **2b.** The splitting between singularities is shown. The second and fourth columns present the calculated static ^{13}C line shape employing the ^{13}C δ_{ii} values collected in Table 2. The span Ω parameters are given inside the spectra. Rows represent samples **1**, **2a**, and **2b**, respectively.

From comparative analysis of the set of data for the $^{1}H-^{13}C$ LG-CP powder pattern and line-shape of ^{13}C static spectra, it is apparent that both techniques are sensitive to the medium range (from micro- to millisecond) molecular motion of phenyl rings of Phe and Tyr residues. The $^{1}H-^{13}C$ Pake doublets for Tyr are different. The value of splitting equal to 12.6 kHz corresponds to a static ring (sample **1**). The slightly lower values for **2a** and **2b** samples suggest a small wobbling of rings but exclude their π flip. This wobbling reduces the span values ca. 25 ppm. The difference of the line shape for **2a** and **2b** related to the distinction of ^{13}C δ_{22} parameters is very likely due to the hydrogen bonding effect.[46] The hydroxyl group of tyrosine for sample **2b** is involved in stronger hydrogen bond interaction compared to **2a**.

The differences in the molecular motion for phenyl rings of Phe are more evident. For sample **1**, the phenyl ring is static. For **2a**, the phenyl ring undergoes π-flip. The value of splitting equal to ca. 7 kHz is typical for this kind of molecular dynamics. The flip of the phenyl ring significantly reduces the chemical shift anisotropy of the CH carbons, which are not aligned on the rotation axis. The difference in Ω span parameters for **1** and **2a** is equal to ca. 50 ppm. Judging from the $^{1}H-^{13}C$ line shape of the Pake doublet, the flip of the phenyl ring of **2a** is slightly different compared to **2b**. The span for **2b** was found to be 174 ppm.

4. CONCLUSIONS

As a part of continuing structural studies of opioid peptides, in this work, results showing the influence of the stereochemistry of the alanine residue on the molecular packing in the crystal lattice and the internal molecular dynamics of the aromatic groups are reported. This study clearly demonstrates that three-peptides and tetra-peptides with L-Ala in the sequence very easily form different crystal modifications. For Tyr-L-Ala-Phe, two forms (ref 16) were found, and, for Tyr-L-Ala-Phe-Gly, three modifications were found (this paper). On the other hand, the peptides with D-Ala do not show such tendencies, although different conditions for crystallization were tested. It seems that one of the factors, which can be important in the preorganization mechanism anticipating the formation of crystals, is the intramolecular CH$-\pi$ interaction between aromatic rings of tyrosine and phenylalanine and the methyl group of alanine. Such an interaction is possible only for the D-Ala residue. For L-Ala in the peptide sequence, the methyl group is aligned on the opposite side with respect at least to one of the aromatic groups. It can be further speculated that such internal CH$-\pi$ contacts can also occur during the interaction of ligand−receptor, making the message sequence of opioid peptides more rigid and finally selective. The dynamic processes, which are the result of different arrangements of molecules in the crystal lattice, are evident. Employing different solid state NMR methodologies, both the time-scale of molecular motions and their geometry can be followed. Knowledge concerning dynamic processes of natural products is crucial not only to understand their biological activity but also in cases when X-ray coordinates are used for theoretical calculations of NMR shielding parameters and structure assignment in the solid state.[47]

AUTHOR INFORMATION

Corresponding Author

*E-mail address: marekpot@cbmm.lodz.pl.

ACKNOWLEDGMENT

The authors are grateful to the State Committee for Scientific Research (MNiSW) for financial support, Grant No. N N204 1313 35.

REFERENCES

(1) Olson, G. A.; Olson, R. D.; Kastin, A. J.; Coy, D. H. *Peptides* **1982**, *3*, 1039.
(2) Hughes, J.; Smith, T. W.; Kosterlitz, H. W.; Fothergill, L. A.; Morgan, B. A.; Morris, H. R. *Nature* **1975**, *258*, 577.
(3) Thematic Issue, *Curr. Top. Med. Chem.* **2004**, *4*, 1.
(4) Kreil, G.; Barra, D.; Simmaco, M.; Erspamer-Falconieri, G.; Melchiorri, P.; Negri, L.; Severini, C.; Corsi, R.; Melchiorri, P. *Eur. J. Pharmacol.* **1989**, *162*, 123.
(5) Erspamer, V.; Melchiorri, P.; Erspamer-Falconieri, G.; Melchiorri, P.; Negri, L.; Corsi, R.; Severini, C.; Barrat, D.; Simmacot, M.; Kreil, G. *Proc. Natl. Acad. Sci. U.S.A.* **1989**, *86*, 5188.
(6) Richter, K.; Egger, R.; Kreil, G. *Science* **1987**, *238*, 200.
(7) Jilek, A.; Kreil, G. *Monatsh. Chem.* **2008**, *139*, 1.
(8) Schwyzer, R. *Biochemistry* **1986**, *25*, 6335.
(9) Spadaccini, R.; Temussi, P. A. *Cell. Mol. Life. Sci.* **2001**, *58*, 1572.
(10) Castiglione-Morelli, M. A.; Lelj, F.; Pastore, A.; Salvadori, S.; Tancredi, T.; Tomatis, R.; Trivellone, E.; Temussi, P. A. *J. Med. Chem.* **1987**, *30*, 2067.

(11) Temussi, P. A.; Picone, D.; Tancredi, T.; Tomatis, R.; Salvadori, S.; Marastoni, M. *FEBS Lett.* **1989**, *247*, 283.
(12) Balboni, G.; Marastoni, M.; Picone, D.; Salvadori, S.; Tancredi, T.; Temussi, P. A. *Biochem. Biophys. Res. Commun.* **1990**, *169*, 617.
(13) Temussi, P. A.; Picone, D.; Saviano, G.; Amodeo, P.; Motta, A.; Tancredi, T.; Salvadori, S.; Tomatis, R. *Biopolymers* **1992**, *32*, 367.
(14) Amodeo, P.; Motta, A.; Tancredi, T.; Salvadori, S.; Tomatis, R.; Picone, D.; Saviano, G.; Temussi, P. A *Pept. Res.* **1992**, *4*, 48.
(15) Słabicki, M. M.; Potrzebowski, M. J.; Bujacz, G.; Olejniczak, S.; Olczak, J. *J. Phys. Chem. B* **2004**, *108*, 4535.
(16) Trzeciak-Karlikowska, K.; Bujacz, A.; Jeziorna, A.; Ciesielski, W.; Bujacz, G. D.; Gajda, J.; Pentak, D.; Potrzebowski, M. J. *Cryst. Growth Des.* **2009**, *9*, 4051.
(17) Castiglione-Morelli, M. A.; Salvadori, S.; Tancredi, T.; Trivellone, E.; Balboni, G.; Marastoni, M.; Tomatis, R.; Temussi, P. A. *Biopolymers* **1988**, *27*, 1353.
(18) Brook, M. A.; Chan, T. H. *Synthesis* **1983**, 201.
(19) Sheldrick, G. M.; Kruger, G. M.; Goddard, R. SHELXS-86, Structure Solution Program. *Acta Crystallogr., Sect. A: Found. Crystallogr.* **1990**, *A46*, 467.
(20) Sheldrick, G. M. *SHELXL-93, Program for Crystal Structure Refinement*; University of Göttingen: Göttingen, Germany, 1993; p 63.
(21) Morcombe, C. R.; Zilm, K. W. *J. Magn. Reson.* **2003**, *162*, 479.
(22) Metz, G.; Wu, X.; Smith, S. O. *J. Magn. Reson., Ser. A* **1994**, *110*, 219.
(23) Bennett, A. W.; Rienstra, C. M.; Auger, M.; Lakshmi, K. V.; Griffin, R. G. *J. Chem. Phys.* **1995**, *103*, 6951.
(24) *TopSpin*, version 2.1; Bruker BioSpin GmbH: Rheinstetten, Germany, 2007.
(25) Antzutkin, O. N.; Shekar, S. C.; Levitt, M. H. *J. Magn. Reson., Ser. A* **1995**, *115*, 7.
(26) (a) Vinogradov, E.; Madhu, P. K.; Vega, S. *Top. Curr. Chem.* **2005**, *246*, 33. (b) Schnell, I.; Spiess, H. W. *J. Magn. Reson.* **2001**, *151*, 153. (c) Brown, S. P. *Macromol. Rapid Commun.* **2009**, *30*, 688.
(27) (a) Kamihira, M.; Naito, A.; Nishimura, K.; Tuzi, S.; Saito, H. *J. Phys. Chem. B* **1998**, *102*, 2826. (b) Kamihira, M.; Naito, A.; Tuzi, S.; Saito, H. *J. Phys. Chem. A* **1999**, *103*, 3356.
(28) Krushelnitsky, A.; Reichert, D. *Prog. NMR Spectrosc.* **2005**, *47*, 1.
(29) Alla, M.; Lippmaa, E. *Chem. Phys. Lett.* **1976**, *37*, 260.
(30) Opella, S. J.; Frey, M. H. *J. Am. Chem. Soc.* **1979**, *101*, 5854.
(31) Zilm, K. W. In *Spectral Editing Techniques: Hydrocarbon Solids, Encyclopedia of NMR*; Grant, D. M., Harris, R. K., Eds.; John Wiley & Sons Ltd.: Chichester, U.K., 1996; Vol. 7, p 4498.
(32) Ladizhansky, V. *Solid State Nucl. Magn. Reson.* **2009**, *36*, 119.
(33) Wylie, B. J.; Rienstra, C. M. *J. Chem. Phys.* **2008**, *128*, 052207.
(34) Drobny, G. P.; Long, J. R.; Karlsson, T. *Annu. Rev. Phys. Chem.* **2003**, *54*, 531.
(35) Schmidt-Rohr, K.; Spiess, H. W. *Multidimensional Solid-State NMR and Polymers*; Academic Press: London, 1994.
(36) Cobo, M. F.; Malinakova, K.; Reichert, D.; Saalwachter, K.; Deazevedo, E. R. *Phys. Chem. Chem. Phys.* **2009**, *11*, 7036.
(37) Ladizhansky, V.; Vega, S. *J. Chem. Phys.* **2000**, *112*, 7158.
(38) Ramamoorthy, A.; Wei, Y.; Lee, D. K. *Annu. Rep. NMR Spectrosc.* **2004**, *52*, 1.
(39) Hong, M.; Yao, X.; Jakes, K.; Huster, D. *J. Phys. Chem. B* **2002**, *106*, 7355.
(40) Lorieau, J.; McDermott, A. E *Magn. Reson. Chem.* **2006**, *44*, 334.
(41) (a) DeAzevedo, E. R.; Bonagamba, T. J.; Reichert, D. *Prog. NMR Spectrosc.* **2005**, *47*, 137. (b) Saito, H.; Ando, I.; Ramamoorthy, A. *Prog. NMR. Spectrosc.* **2010**, *57*, 181and references cited therein.
(42) Spiess, H. W. *Colloid Polym. Sci.* **1983**, *261*, 193.
(43) (a) Hu, J.; Wang, W.; Liu, F.; Solum, M. S.; Alderman, D. W.; Pugmire, R. J. *J. Magn. Reson., Ser. A* **1995**, *113*, 210. (b) Alderman, D. W.; McGeorge, G.; Hu, J. Z.; Pugmire, R. J.; Grant, D. M. *Mol. Phys.* **1998**, *95*, 1113. (c) Frydman, L.; Chingas, G. C.; Lee, Y. K.; Grandinetti, P. J.; Eastman, M. A.; Barral, G. A.; Pines, A. *J. Chem. Phys.* **1992**, *97*, 4800. (d) Kolbert, A. C.; Griffin, R. G. *Chem. Phys. Lett.* **1990**, *166*, 87.
(44) Wei, Y.; Lee, D-K; McDermott, A. E.; Ramamoorthy, A. *J. Magn. Reson.* **2002**, *158*, 23.
(45) Dixon, W. T. *J. Chem. Phys.* **1982**, *77*, 1800.
(46) Wei, Y.; Lee, D.-K.; Ramamoorthy, A. *J. Am. Chem. Soc.* **2001**, *123*, 6118.
(47) De Gortari, I.; Portella, G.; | Salvatella, X.; Bajaj, V. S.; van der Wel, P. C. A.; Yates, R.; Segall, M. D.; Pickard, C. J.; Payne, M. C.; Vendruscolo, M. *J. Am. Chem. Soc.* **2010**, *132*, 5993.